

# Helical Pile Installation for Offshore Renewable Energy Exploration in Clay Seabed

Y. Hu<sup>1</sup>, M. Zhang<sup>2</sup> and S. N. Ullah<sup>3</sup>

<sup>1</sup>Professor in Geotechnical Engineering, School of Engineering, The University of Western Australia, Email: [yuxia.hu@uwa.edu.au](mailto:yuxia.hu@uwa.edu.au)

<sup>2</sup>PhD Candidate, School of Engineering, The University of Western Australia, Email: [meili.zhang@research.uwa.edu.au](mailto:meili.zhang@research.uwa.edu.au)

<sup>3</sup>Senior Lecturer, School of Engineering and Technology, Central Queensland University, Email: [s.ullah@cqu.edu.au](mailto:s.ullah@cqu.edu.au)

## ABSTRACT

Offshore wind and wave energy exploration are moving from shallow waters with fixed foundations to deep waters with floating devices. Helical pile has the potential to be used as both shallow water foundations and deep water anchors due to its 'quiet' installation and environmental friendliness to marine living systems. Although helical pile and/or anchor have been used extensively for onshore applications, their offshore applications need larger diameters and longer shaft than the onshore counterparts hence pose significant installation challenges. This paper presents the current studies on helical pile installation process in clay seabed. The installation of helical pile in uniform and normally consolidated clay have been studied physically in centrifuge and numerically using large deformation finite element (LDFE) analyses. Both installation torque and installation force (or crown force) were studied under different pile-soil friction coefficients and different helical pile advancement ratios (AR: ratio of pile penetration to helix pitch). Soil flow mechanisms under different ARs can explain the development of required torque and crown force during torsional pile installation. The installation torque and installation force are a function of AR and can be designed based on the capacity of installation equipment.

**Keywords:** helical anchor, clay seabed, offshore energy, numerical analysis, installation, capacity

## 1 INTRODUCTION

Offshore renewable energy exploration, such as wind and wave energy, is moving from shallow waters with fixed foundations to deep waters with floating devices (Figure 1). To secure these fixed and floating devices, the design of economical and environmentally friendly foundation/anchor systems is vitally important. Among all different foundation and anchor options, such as monopile, drag anchor, plate anchor and pile anchor, helical pile is attracting more and more attention due to its quieter installation with less noise emission into the ocean environment as the installation noise may harm marine lives.

Helical pile has been applied to support marine and onshore structures for a few decades. Its early application was offshore in shallow waters in the 1950s for developments in marine environment (Feld, 1953). However, over the last few decades, the development of helical piles/anchors application was largely to support onshore structures, such as transmission towers, billboard lights and sign foundations (Lutenegger, 2017). The onshore helical piles/anchors generally have small shaft diameters in

the range of 0.0138 m ~ 0.51 m. The helix diameter is in the range of 0.15 m ~ 0.9 m. Table 1 shows a few examples of onshore helical piles in soils with fine particles. Even to support a large residential building with 11-storeys, the helical piles had a shaft diameter of 0.05 m and their helix diameters varied from 0.2 m to 0.3 m. (Vito & Cook, 2011).

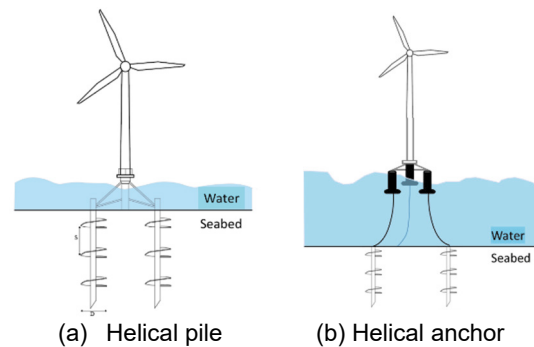


Figure 1. Offshore wind turbine with helical pile and anchor foundations

Table 1: Samples of recent studies of onshore helical piles in silt and clay

| Researcher          | Year | Location                              | Ground Condition                             | Shaft Diameter d (m) | Helix Diameter D (m) |
|---------------------|------|---------------------------------------|--|----------------------|----------------------|
| Sakr                | 2011 | Field tests, Alberta, Canada          | Sand, stiff glacial till                     | 0.32-0.51            | 0.76-1.02            |
| Vito & Cook         | 2011 | 11-storey building, Ontario, Canada   | Sandy silt, silt                             | 0.051                | 0.2-0.3              |
| Weech & Howie       | 2012 | Field tests, British Columbia, Canada | Peat, deltaic clayey silt, marine silty clay | 0.089                | 0.356                |
| Papadopoulou et al. | 2014 | FE, Plaxis 2D                         | Sand and clay                                | 0.076                | 0.22                 |
| Alwalan & Naggari   | 2020 | FE, Plaxis 2D                         | Sand and clay                                | 0.324                | 0.61                 |

The helical piles designed for offshore renewable energy explorations need larger shaft and helix diameters than their onshore applications. This is because the offshore structures are experiencing larger environmental loadings, such as wind, wave and current, and structural loading as offshore structures are larger and heavier than the onshore ones. Due to the large size of offshore helical piles, the torsional installation offshore can be challenging.

This paper presents some development in the helical pile research in clay seabed. The studies include physical model tests using centrifuge and numerical analysis using LDFE. The required torque and crown force were investigated for optimum installation designs against pile advancement ratio.

## 2 CENTRIFUGE TESTS

### 2.1 Model pile - 1

The helical pile in normally consolidated (NC) clay was tested in centrifuge under 50g (Ullah et al., 2019). The model pile has three helices (Figure 1) and the installation torque and crown force were measured in four locations to investigate the distribution of each helix during installation. The pile was installed with a constant crown force. Its advancement ratio was estimated as  $AR = 1.0$ , which means the pile penetrates one pitch per revolution. Soil undrained shear strength profile, pile dimensions and sensor locations are also shown in Figure 2.

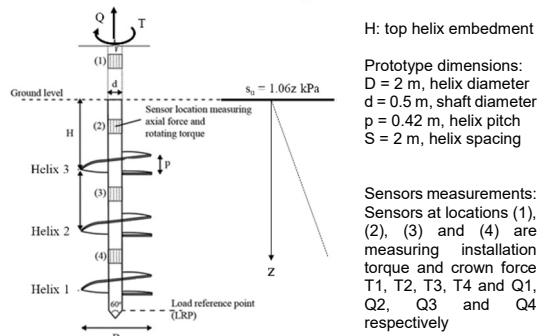


Figure 2. Model pile - 1 in centrifuge test

### 2.2 Centrifuge test results

The pile was installed in NC clay. The normalised installation responses are displayed in Figure 3. As  $s_u = 1.06z$  kPa, the average  $s_{ua} = 4.24$  kPa over the pile penetration of 8 m is used in normalisation. Positive  $Q$  and  $T$  are defined in the figure. The penetration depth is recorded for the reference point (RP). The crown forces are compressive from all sensors. It can be seen that the total installation force has  $Q1 \approx Q2$  in Figure 3a, as there is no extra helix between these points (1) and (2). The shaft between these two points has minimum effect due to its small diameter and soft soil near the surface. The crown force of  $Q4$  from Helix 1 is developing tensile force with penetration depth. This means that, with  $AR = 1.0$ , the rotation of the bottom helix can generate tensile force after it is fully embedded in soil. This phenomenon can also be

observed when Helix 2 is fully embedded in soil. This is interesting, as this phenomenon shows less reliance on the crown force during installation.

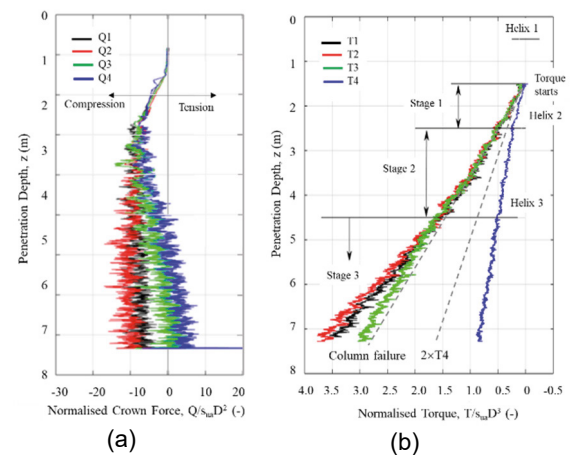


Figure 3. Individual helix effects on installation torque and force of model pile-1 under constant crown force

Figure 3b shows the development of installation torque with pile penetration. The torque  $T4$  measures the torque resistance from Helix 1 and it increases linearly with penetration depth as the soil strength increases linearly with soil depth. However, as Helix 2 enters the soil, the total torque from Helices 1&2 (i.e.  $T3$ ) is more than double the  $T4$  (i.e.  $T3 > 2 \times T4$ ). This means that Helices 1&2 are not working as two individual helices. This is consistent with other research findings that the spacing between two helices needs to be  $S/D \geq 3$  (Alwalan & Naggar, 2020) for individual helix behaviours. The helix spacing here is  $S/D = 1.0$ , hence a soil column failure between the bottom two helices is expected. The estimated torque resistance from the column failure matches the measured  $T3$  fairly well. The  $T1$  &  $T2$  are slightly higher than  $T3$ , as the Helix 3 embedded in top soil with low strength. At the same time, the torque resistance from the shaft between sensor points (1) and (2) is minimum, due to small shaft and soft surface soil.

## 3 LARGE DEFORMATION FE ANALYSIS

### 3.1 Model pile - 2

To study a single helix contribution to the installation torque and crown force, a pile with a single helix is analysed in a uniform clay. Figure 4 shows the helical pile dimensions and soil strength profile. The definitions of all variables are listed in Figure 4 for easy reference.

### 3.2 Large deformation FE analysis

The torsional installation of the helical pile is simulated using 3D large deformation finite element (LDFE) analysis with coupled Eulerian Lagrangian (CEL) method in ABAQUS (2011). The FE model set-up is depicted in Figure 3. The pile shaft and helix plate are modelled as a rigid Lagrangian body and the soil domain is discretised using 8-node brick elements

(EC3D8R). The mesh is refined around the helical shaft and helix plate with minimum element size of  $D/40$ . The soil domain is set large enough to avoid boundary effect (see Figure 5).

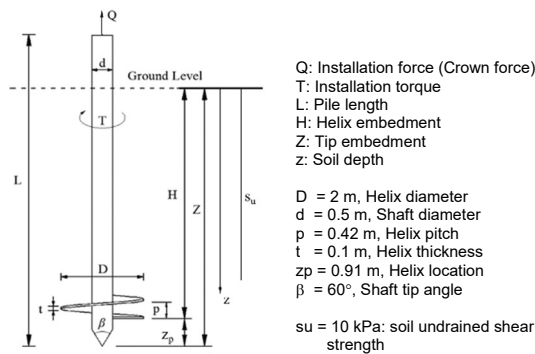


Figure 4. Model pile – 2 in LDFE analysis

The soil is modelled as a medium soft uniform clay with its undrained shear strength of  $s_u = 10$  kPa. The soil Young’s modulus is set as medium stiff clay of  $E_s/s_u = 500$ , which is commonly used to simulate offshore clays (Hu et al., 1999). The Poisson ratio of  $\nu_s = 0.49$  and friction and dilation angles of  $\phi = \psi = 0$  are set up for undrained analysis. Soil submerged density is  $\rho_s = 700$  kg/m<sup>3</sup>.

The helical pile is simulated as a weightless rigid body. The interface friction between soil and pile varies as  $\alpha = 0 \sim 1.0$ , where  $\alpha = 0$  is fully smooth and  $\alpha = 1.0$  is fully rough.

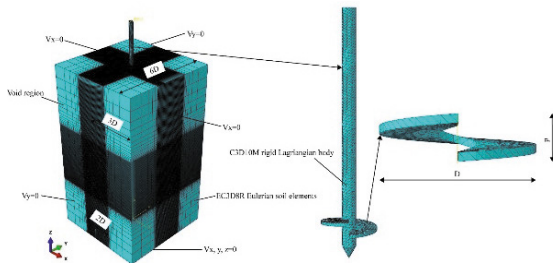


Figure 5. 3D LDFE model of model pile - 2

### 3.3 LDFE/CEL model validation

The LDFE/CEL model is validated against centrifuge test data using model pile – 1 in Figure 2 (Ullah et al., 2022). The LDFE/CEL results are compared with centrifuge test data of total resistant torque (i.e. T1 in Figure 3). It can be seen that the numerical results agree well with the centrifuge test data. The slight over estimations of the numerical result may be due to the strain-softening effect of centrifuge clay (i.e. clay sensitivity  $S_t = 3$ , Ullah & Hu, 2020), which is not considered in the numerical analysis. However, the torque from the numerical analysis shows the same trend as that from the centrifuge test.

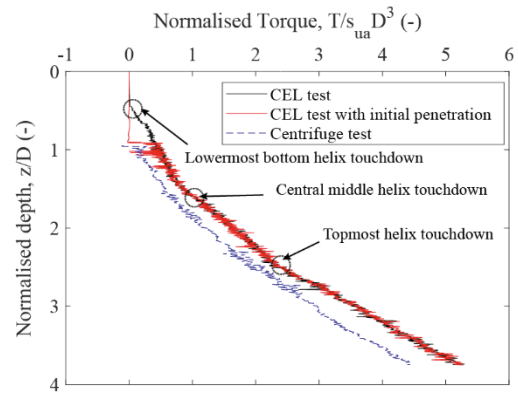


Figure 6. LDFE/CEL mode validation of model pile – 1 in centrifuge test

### 3.4 Numerical analysis result

In this study, the effects of helical pile friction and pile advancement ratio on the installation torque and crown force are studied. The advancement ratio (AR) of the helical pile is defined as

$$AR = \text{vertical displacement per revolution}/p \quad (1)$$

where AR = 1.0 is neutral rotation (i.e. one pitch vertical displacement per revolution); AR < 1 is over rotation (i.e. fast rotation/slow penetration) and AR > 1 is under rotation (i.e. slow rotation/fast penetration).

#### Pile friction effect

The pile friction effect at AR = 1.0 and  $s_u = 10$  kPa is displayed in Figure 7. It can be seen that, under neutral rotation, the crown force is compressive. With increasing penetration depth, the compressive crown force is decreasing in magnitude. This means that, at AR = 1.0, the helix is generating tensile force, which is similar to the observations in the centrifuge test (see axial force Q4 in Figure 3a). The pile friction has minimum effect on the crown force at  $\alpha = 0 \sim 0.45$  (Figure 7a), where common friction coefficient lies for steel piles.

However, the pile friction has profound effect on installation torque. The torque increases linearly with increasing friction coefficient  $\alpha$  (Zhang et al., 2022). A formula was developed by Zhang et al. (2022) to calculate the torque as a function of  $z/D$  and  $\alpha$ .

It is apparent that the required installation torque and crown force can be minimised when the pile is relatively smooth.

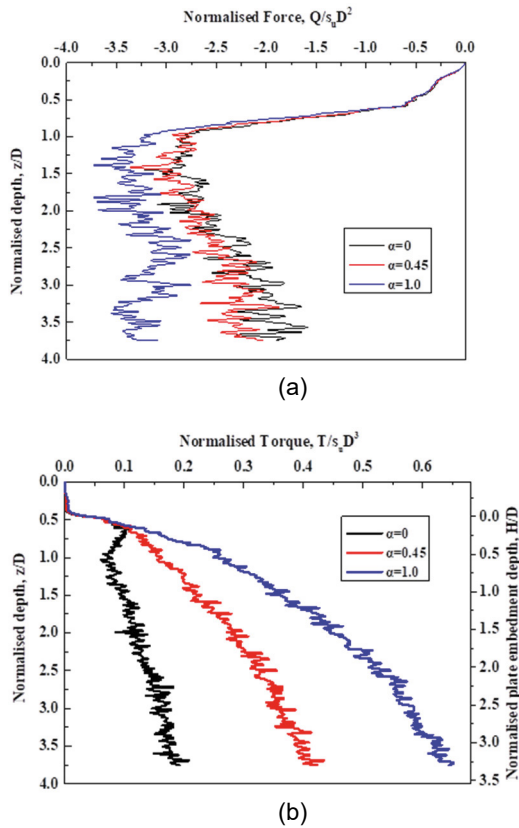


Figure 7. Pile friction effect ( $AR = 1.0$ ,  $s_u = 10$  kPa)

**Advancement ratio (AR) effect**

The effect of pile advancement ratio is depicted in Figure 8. It is interesting to see that, when the helical pile is over rotating (i.e.  $AR < 1.0$ , fast rotation/slow penetration), the crown force changes from compression to tension, as it is also observed in centrifuge tests. (i.e. Q4 in Figure 3a). On the contrary, when the pile is under rotation (i.e.  $AR > 1.0$ , the pile is pushed into soil with faster penetration than rotation), hence the crown force increases with increasing pile penetration depth until a constant crown force is reached at  $z/D = 2.5$ . Thus, it is desirable to install the helical pile with  $AR \leq 1.0$  (i.e. over rotation).

However, with  $AR \leq 1.0$ , the required installation torque becomes higher under neutral and over rotation. Thus, the crown force can be reduced by increasing installation torque.

By correlating the crown force graph to the torque graph in Figure 8, there is a potential to provide an optimal installation design, based on the installation equipment capacity. Figure 9 shows the preliminary design chart based on pile installation AR. The required crown force and torque during helical pile installation are data in Figure 8 at  $z/D = 3.5$ .

**Example 1:** minimising required crown force (i.e.  $Q \sim 0.0$ , A→B). From  $Q = 0.0$  at point A, the required is  $AR = 0.84$ , where  $T/s_u D^3 = 0.45$  at point B. Thus, the required installation torque can be estimated.

**Example 2:** under allowable installation torque of  $T/s_u D^3 = 0.3$ , C→D. From the allowable  $T/s_u D^3$  at point

C, the required is  $AR = 1.19$ , where the required crown force is  $Q/s_u D^2 = 4.2$  at point D. Then the required crown force can be calculated.

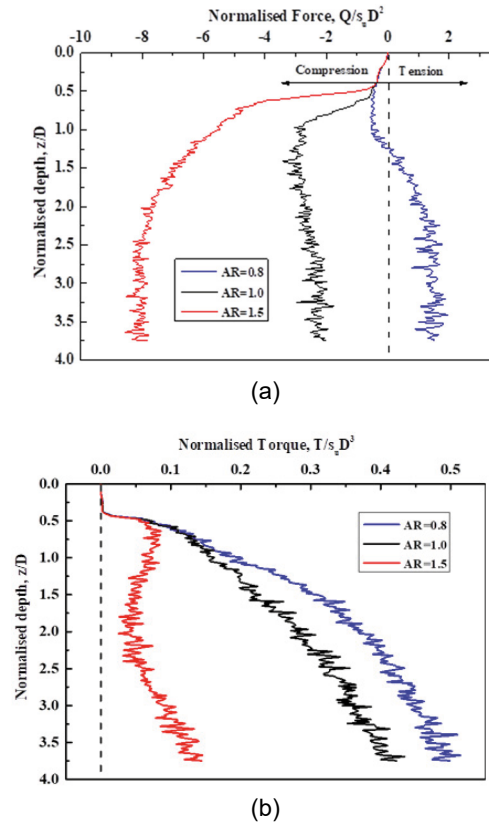


Figure 8. Pile advancement ratio effect ( $\alpha = 0.45$ )

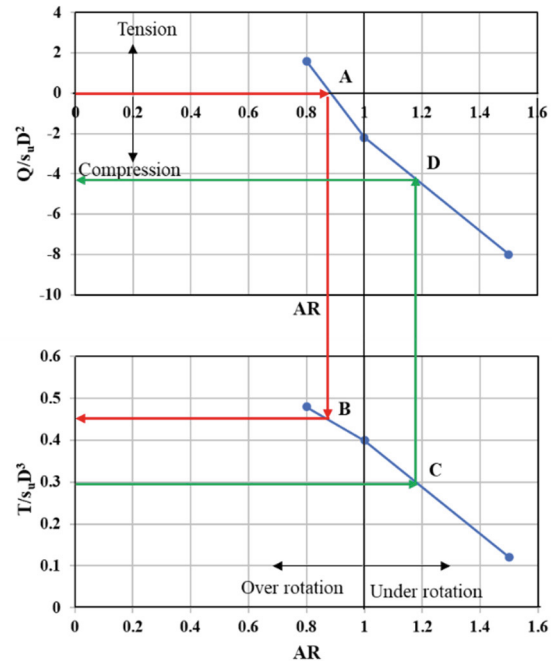


Figure 9. Required crown force and torque at  $\alpha = 0.45$ ,  $z/D = 3.5$

### 3.5 Soil flow mechanisms at various AR

The soil flow mechanisms during helical pile installation in a uniform clay are depicted in Figure 10. It can be seen that, under neutral rotation of AR = 1.0 in Figure 10b, the soil flow is localised around the top and bottom ends of the pitch. However, with over rotation of AR = 0.8 (i.e. fast rotation/slow penetration), the soil around the helix brim is flowing from the top of the helix downwards. This indicates a tensile force is generated, since a horizontal plate subjected to upwards tensile force can induce soil flowing from top to bottom of the plate around the brim. On the other hands, with under rotation of AR = 1.5 (i.e. slow rotation/fast penetration), the soil around the brim is flowing from the bottom of the helix upwards. This is a typical soil flow mechanism when a horizontal plate penetrates into clays with a compressive force (Song et al., 2008).

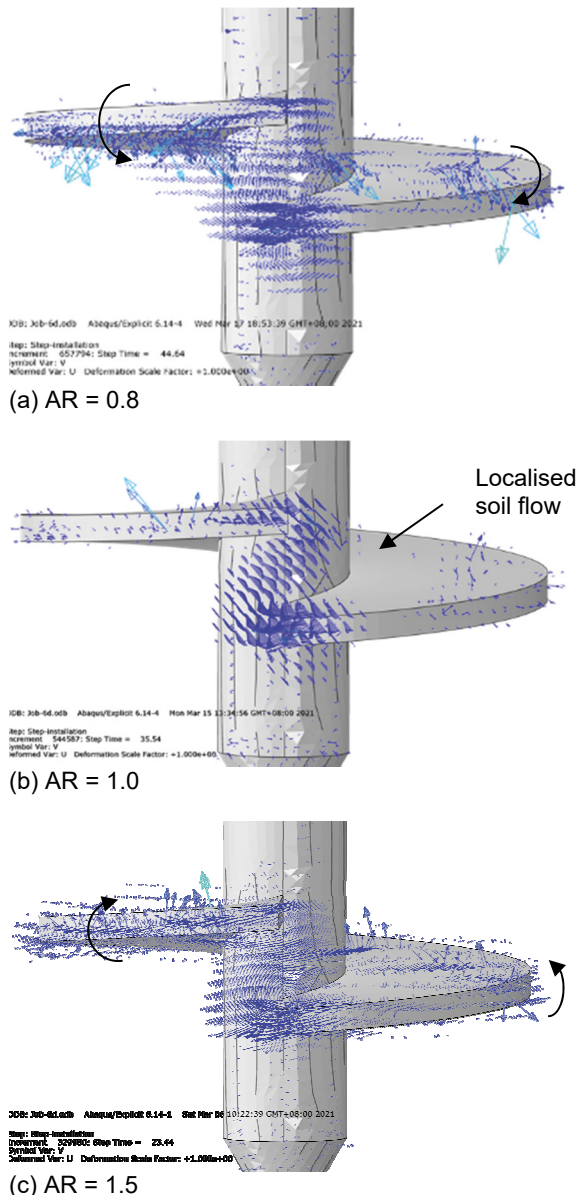


Figure 10. Soil flow mechanisms during helical pile installation with  $\alpha = 0.45$  and  $s_u = 10$  kPa

## 4 CONCLUSION

This paper presents current studies on the helical pile installation in clay seabeds in centrifuge test and by LDFE/CEL numerical analysis. In the centrifuge test, a triple helices pile was installed in a NC clay. In the numerical analysis, a single helix pile was installed in a uniform clay, after the numerical method was validated against the centrifuge test data.

In the centrifuge test, it was found that the bottom two helices played a major role in crown force and installation torque development. A clear tensile force was generated by the bottom two helices. The bottom two helices were acting together to form a column failure to resist torque.

In the numerical analysis, the pile friction had minimum effect on the crown force when  $\alpha = 0\sim 0.45$ . However, the pile friction had a strong effect on installation torque, where the installation torque increased linearly with the friction coefficient.

The pile advancement ratio played a major role in the development of crown force and installation torque during the rotational installation of a helical pile. Under rotation was not recommended due to high crown force requirement. Neutral and over rotation can be designed based on the installation equipment capacity.

More analyses are underway to establish a full design chart to guide helical pile installations in clay.

## REFERENCES

- ABAQUS (2011), "ABAQUS user's and theory manuals.", version 6.11, ABAQUS Inc.
- Alwalan, M.F., and El Naggari, M.H. (2020). "Finite element analysis of helical piles subjected to axial impact loading." *Computers and Geotechnics*, 123(2020), 103597.
- Feld, J. (1953). "A historical chapter: British royal engineers' papers on soil mechanics and foundation engineering, 1837-1874." *Geotechnique*, 3(6), 242-247.
- Hu, Y., Randolph, M.F. and Watson, P.G., (1999). "Bearing response of skirted foundation on nonhomogeneous soil", *J. Geotechnical and Geoenvironmental Engr., ASCE*, 125(11), 924-935.
- Lutenegger, A. J. (2011). "Historical development of iron screw-pile foundations: 1836 – 1900.", *Int. Journal for the History of Engineering and Technology*, 81(1), 108-128.
- Lutenegger, A. J. (2017). "Support of offshore structures using helical anchors." 8th Int. Conf. Offshore Site Investigation Geotechnics, SUT, 995(1004), 995-1004.
- Papadopoulou, K., Saroglou, H., and Papadopoulou, V. (2014). "Finite element analyses and experimental investigation of helical micropiles." *Geotechnical and Geological Engineering*, 32(4), 949-963.
- Sakr, M. (2012). "Installation and performance characteristics of high capacity helical piles in cohesive soils." *Journal of Deep Foundations Institute – DFI*, 6(1), 41-57.
- Song, Z., Hu, Y., and Randolph, M.F. (2008). "Numerical simulation of vertical pullout of plate anchors in clay". *Journal of Geotechnical and Geoenvironmental Engineering, ASCE*, 134(6), 866-876.
- Ullah, S.N., and Hu, Y. (2020). "Discussion: A review on the behaviour of helical piles as a potential offshore foundation system." *Marine Georesources & Geotechnology*, 38(9), 1121-1127.

- Ullah, S.N., Hu, Y., and O'Loughlin, C. (2019). "A green foundation for offshore wind energy-helical piles." World Engineers Convention 2019, WEC2019, 272-285.
- Ullah, S.N., Hu, Y., and O'Loughlin, C. (2022). "Torsional installation and vertical tensile capacity of helical piles in clay." *Geotechnique* (in press).
- Vito, D., and Cook, T. (2011). "Highly loaded helical piles in compression and tension applications: a case study of two projects." 2011 Pan-Am CGS Geotechnical Conference.
- Weech, C.N., and Howie, J.A. (2012). "Helical piles in soft sensitive soils – A field study of disturbance effects on pile capacity." VGS Symposium on Soft Ground Engineering.
- Zhang, M., Hu, Y., Ullah, S.N., and Yu, L. (2022). "Frictional effect of helical pile installation in uniform clays." The 32nd Int. Ocean and Polar Engn. Conf. (ISOPE-2022), June 2022, Shanghai, China, ISOPE22-089, 1486-1474.